RSC Advances

ROYAL SOCIETY OF CHEMISTRY

www.rsc.org/advances

ARTICLE TYPE www. rsc.org/xxxxxx | XXXXXXXX

Photocatalytic NO_x abatement: Why the selectivity matters

Jonathan Z. Bloh,[a,‡] Andrea Folli,[a,b] and Donald E. Macphee*[a]

Received Xth XXXXXXXXXX 20XX, Accepted Xth XXXXXXXXX 20XX
First published on the web Xth XXXXXXXXXX 200X
DOI: 10.1039/b000000x

Titanium dioxide photocatalysis offers an excellent way to oxidise NO_x to nitrate and thus reduce air pollution. However, unmodified titanium dioxide also releases a significant amount of the toxic intermediate nitrogen dioxide in the process, a problem that is rarely discussed in previous literature. Herein, we highlight this issue by presenting systematic data on the activity and selectivity of a number of commercial titania powders. The photocatalytic performance of a previously developed W/N-codoped titanium dioxide is also reported which, for the first time, offers a way to eliminate this problem as it exhibits an exceptionally high selectivity towards nitrate. The selectivity appears to be solely dependent on the tungsten content, a concentration of 4.8 at.% is sufficient to induce a very high selectivity. Furthermore, the high selectivity could also be replicated by a W/N-codoped sample derived from the industrial sulphate synthetic process.
The increased selectivity comes at the expense of absolute activity, which is lower than in the reference titania samples. This raises the question of how to properly evaluate NO_x abatement photocatalysts when there are two factors to consider, activity and selectivity. To resolve this, we propose to define a new figure of merit for the evaluation of NO_x abatement photocatalysts by distilling total NO_x removal and selectivity into one value, the DeNOx index. It is derived by assigning a toxicity value to both NO and NO_2 and then expressing the change in total toxicity rather than the concentration change of the individual nitrogen oxides.
Keywords: Photocatalysis, product spectrum, byproduct, doped titanium dioxide, nitrogen oxide toxicity, DeNOx index.

1 Introduction

Nitrogen oxides, commonly referred to as NO_x, are a group of different compounds that play a major role in atmospheric chemistry and air pollution. The term is usually used to refer specifically to nitric oxide (NO) and nitrogen dioxide (NO_2) which are the two most common compounds of this group. Although they are sometimes formed in natural processes such as lightning the majority of NO_x emissions are formed anthropogenically in high-temperature processes where both oxygen and nitrogen are present, *e.g.*, internal combustion engines, gas- or oil-fired heating and industrial furnaces.[1] They constitute a major environmental and health concern as they are toxic compounds and also facilitate the formation of ozone and acid rain.[2,3] As a consequence of this, increasingly stronger regulations and policies are in place enforcing actions to reduce emissions and to lower the overall pollutant levels.[4]

Apart from reducing the emissions directly by optimising the combustion process for low-NO_x formation rates, several other techniques have been developed to reduce the NO_x emission of combustion processes.[5] Among the more widely adopted procedures are selective catalytic or non-catalytic reduction using a reducing agent such as ammonia to reduce the nitrogen oxides to molecular nitrogen. An alternative approach is to absorb and oxidise the nitrogen oxides in aqueous solutions.[1,6] All of these techniques have in common that they need external reagents and maintenance and are only effective when employed directly at the emission source. There are also recent reports questioning the efficacy of the strategy to reduce ambient NO_x levels solely by reducing their emissions.[7,8] Semiconductor photocatalysis presents an appealing alternative capable of removing NO_x and other air pollutants from the air once it has already been released and dispersed.[9] Additionally, photocatalysis needs neither maintenance nor external reagents, since the only required reagents are sunlight and molecular oxygen, which are both already present in outdoor conditions.

Owing to these advantageous properties, photocatalysis has been explored as a way to functionalise building materials to give them air cleaning properties.[10–18] Titanium dioxide based photocatalysts supported on cement-based construction materials for the reduction of nitrogen oxide pollution has been investigated extensively not just at the laboratory scale but also in several real-life pilot projects.[19–23] This highlights that this technology is on the verge of being employed on a large scale in the environment. However, the fundamental reaction mech-

† Electronic Supplementary Information (ESI) available: XRD patterns of the synthesised samples. See DOI: 10.1039/b000000x/

[a] *University of Aberdeen, Department of Chemistry, Meston Walk, Aberdeen AB24 3UE, United Kingdom.; E-mail: d.e.macphee@abdn.ac.uk*
[b] *Danish Technological Institute, Gregersensvej 4, 2630 Taastrup, Denmark.*
‡ *Present address: DECHEMA Research Institute, Theodor-Heuss-Allee 25, 60486 Frankfurt am Main, Germany.; E-mail: bloh@dechema.de*

anism of the nitric oxide oxidation, as well as the spectrum and fate of the reaction products, are still only poorly understood.

Up to now, the selectivity of the photocatalytic reaction has only been of interest for applications in organic synthesis.[24,25] In applications focused on the removal of pollutants from various sources, however, usually only the disappearance of the substrate was considered and the selectivity of the reaction and the spectrum of products largely ignored. More recently, the selectivity has attracted some attention and several authors have highlighted that one of the main aspects of the next generation of photocatalysts should be their selectivity.[26–31] This is especially true in the case of photocatalytic removal of nitrogen oxides from the air as during the eventual oxidation of the nitrogen oxides to nitrate there are several toxic intermediate products, the release of which could be detrimental to the air quality. An improvement in the air quality can only be guaranteed by a selective catalyst which suppresses the formation and the release of these undesired intermediates.

Herein, we present a detailed description of the photocatalytic nitric oxide oxidation, its possible intermediate products and their individual hazards. Moreover, a new figure of merit for NO_x abatement photocatalysts, the *DeNOx index* is introduced, which takes account of both activity and selectivity in a single value. This index attempts to depict how a photocatalyst will alter the overall air quality through the removal and formation of the various nitrogen oxides. We also present the NO_x abatement performance of several commercial titania powders as well as a recently developed W/N-codoped titanium dioxide, which contrary to ordinary titanium dioxide exhibits exceptionally high selectivity.

2 Experimental Section

Synthesis and characterisation

Samples of pristine, nitrogen- or tungsten-doped, and tungsten-nitrogen-codoped titanium dioxide were prepared as already described previously.[32] Briefly, for a typical synthesis, 10 mL of titanium isopropoxide ($\geq 97\,\%$, Sigma-Aldrich), were dissolved in 10 mL of anhydrous ethanol. After thoroughly mixing the solution, 5 mL of deionised water (18 MΩ cm) were slowly added to the solution. The resulting white precipitate redissolved upon further stirring. In the next step, 20 mL of a pH 10 ammonia/ammonium chloride buffer (5 % ammonia, Sigma-Aldrich) for the nitrogen containing samples or 20 mL of deionised water for the nitrogen free samples were added to the solution. Finally, the desired amount of ammonium tungstate (BDH Chemicals) or tungstic acid (Hopkin & Williams) was dissolved in 10 mL of warm deionised water and subsequently added to the solution. After thorough stirring for at least 4 h, the solution was filtered, washed several times with deionised water and then dried at 60 °C for 4 h. The dry powders were ground in an agate mortar and then transferred into a crucible for calcination. The samples were calcined either at 400 °C or 600 °C for 4 h and ground again afterwards. Samples of Aeroxide P25 and P90 (Evonik Degussa, Germany), Hombikat UV100, PC50, PC105 and PC500 (Cristal Global), a pure rutile powder (Sigma-Aldrich) and a W/N-codoped titania (PC7A, Huntsman Pigments) were used as received. Brookite nanoparticles were prepared by a procedure reported by Kandiel et al.[33,34] Briefly, 22.2 mL of titanium bis(ammonium lactate) dihydroxide (TALH) aqueous solution (50 %, Sigma-Aldrich) was mixed with 200 mL of 6 mol L^{-1} urea solution. The solution was transferred into a Teflon-lined steel autoclave and heated to 160 °C for 24 h after which it was cooled to room temperature in air. The resulting powder was separated by centrifugation, washed three times with deionised water and dried at 60 °C overnight. Finally, the powder was calcined at 400 °C for 4 h and ground in an agate mortar afterwards. This material was confirmed as 100 % brookite by X-ray diffraction with Rietveld refinement, *cf.* Figure S1.

X-ray diffraction analysis

X-ray diffraction patterns were recorded in the range of 20 to 70 ° 2θ on a Siemens D5000 diffractometer in Bragg-Brentano geometry with CuK$\alpha_{1,2}$ radiation. The resulting patterns were subsequently used for Rietveld refinement using the software PowderCell 2.4. For the refinement anatase, rutile and brookite as well as hexagonal, triclinic and monoclinic tungsten trioxide were taken into account to calculate the phase composition. The XRD patterns can be found in the supporting information, Figure S1-4.

Nitric oxide oxidation

Measurements of the photonic efficiency for the oxidation of nitric oxide were carried out in a glass flow-through reactor where the powder sample were placed on a glass frit inside the reactor so the pollutant gas has to pass through the sample, which is irradiated from above through an optical window. 0.3 g of the samples was uniformly distributed on the circular glass frit with an area of 8.042×10^{-4} m^2 inside the reactor. The pollutant gas, synthetic air with an nitric oxide concentration of 8 ppm and a volumetric flow rate of 8.33×10^{-7} m^3 s^{-1} was then flowed through the reactor. The temperature was controlled using a water jacked around the reactor connected to thermostat and was monitored and kept constant at 27 °C. Prior to entering the reactor, the air was humidified and kept at a constant 42 % relative humidity. The concentrations of NO, NO_2 and total NO_x in the outlet gas flow were monitored using a Thermo Scientific Model 42i-HL High Level NO-NO2-NOX Analyzer (Air Monitors Ltd., United Kingdom). Each

sample was measured in the dark until an equilibrium concentration was reached and afterwards under illumination until steady state concentrations were observed. An Ultra-Vitalux 300 W (Osram, Germany) light source was employed as the light source for irradiation. The resulting photon flux at the position the powder was placed during the experiment was determined using ferrioxalate actinometry[35,36] and was found to be 5.268×10^{-5} mol s^{-1} m^{-2}. Finally, the photonic efficiency ξ, which depicts the ratio of degraded molecules to impinging photons, was calculated according to eq. 1, where c_d is the concentration under dark conditions, c_i the concentration under illumination, $\dot{V}$ the volumetric flow rate, p the pressure, A the irradiated area, R the gas constant, T the absolute temperature and Φ the photon flux impinging the photocatalyst surface as determined by actinometry. The photonic efficiency was determined separately for NO, NO_2 and total NO_x.

$$\xi = \frac{(c_d - c_i) \cdot \dot{V} \cdot p}{\Phi \cdot A \cdot R \cdot T} \quad (1)$$

3 Results

In order to evaluate their suitability as NO_x abatement photocatalysts, several recently developed materials based on W/N-codoped titanium dioxide were tested for their nitric oxide oxidation capabilities. A total of 24 formulations were tested, ranging from 0 to 16.7 at.% tungsten concentration, with and without nitrogen codoping and calcined at either 400 or 600 °C. The physico-chemical properties and band structure of these materials have already been reported in detail elsewhere.[32] In order to put the obtained results into perspective, validate them and to exclude effects originating from the specific synthesis employed here, several commercially available titanium dioxides were also measured and used as standards. These include Aeroxide P25 and P90, UV100, PC50, PC105, PC500 and a pure rutile powder.

The complete oxidation of nitric oxide (NO) to nitrate or nitric acid (NO_3^-/$HONO_2$) in a photocatalytic process is a complex affair that involves several intermediate species and has been previously described in a number of publications.[6,11,37–43] In principle, the photocatalytic oxidation of nitric oxide to nitrate proceeds in three individual one-electron transfer steps, via the intermediate species nitrous acid (HONO) and nitrogen dioxide (NO_2). Each step can be realised by the direct reaction with valence band holes or mediated via reactive oxygen species such as superoxide ($O_2 \cdot^-$), hydrogen peroxide (H_2O_2) or hydroxyl radicals ($\cdot$OH):

$$NO\cdot \xrightarrow{\cdot OH} HONO \xrightarrow{\cdot OH} NO_2\cdot \xrightarrow{\cdot OH} HONO_2 \quad (2)$$

As shown by example in Figure 1, it sometimes takes several hours, depending on the surface area of the sample, for steady state conditions to appear. After reaching that state, however, the observed concentrations were constant for hours. Repeated experiments showed that after several cycles, steady state conditions are reached much faster but with the same final concentrations.

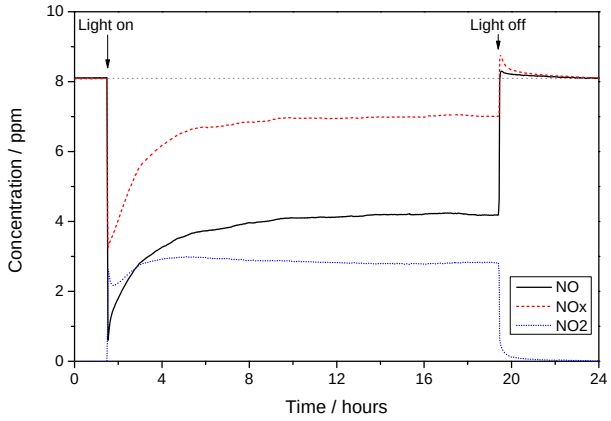

Fig. 1 Exemplary nitric oxide oxidation test for the P25 reference powder under broadband illumination. Displayed are the concentrations for NO (black solid line), NO_2 (blue dotted line) and total NO_x (red dashed line). The point at which the illumination was started and stopped is indicated by the arrows

All of the reference powders that are based on anatase exhibit a very similar behaviour, *cf.* Table 1. The highest degradation rates for nitric oxide are observed with the PC105 powder, closely following by UV100, PC500 and P25. The P90 and PC50 powders are less active by about 30 and 60 %, respectively. When total NO_x is considered rather than just nitric oxide, the removal rates are smaller by a factor of about 3.5 to 4, but the relative ranking remains the same. An exception is the pure rutile powder which shows the lowest activity by far of all the reference powders, only 2 and 8 % of the activity of the worst anatase based catalyst PC50 for NO_x and NO removal, respectively. A pure brookite powder was tested as well for a comparison and it performed comparable with the best anatase based powders in terms of NO removal but at least 30 % better than the best anatase based photocatalyst in terms of NO_x removal, consistent with other reports of brookite's superior photocatalytic activity.[33] The surface area of the samples seems to have a negligible effect on the observed activity, as both the PC500 powder and the P25 powder exhibit approximately the same activity, even though their surface areas are drastically different (350 m^2 g^{-1} for PC500 versus 50 m^2 g^{-1} for P25). This indicates that the activity is rate-limited by the photoreaction rather than the adsorption, as predicted by Dillert el al. for the concentrations applied here.[39]

Similar results were obtained when our own pure titanium dioxide powders were measured (W-0 series). However, af-

ter co-doping with tungsten and nitrogen, the observed photocatalytic activity significantly decreased. The drop in activity appears to be higher for higher tungsten loadings, stabilising after addition of about 1 at.% tungsten, after which no further decrease in activity was observed, even when the tungsten loading was as high as 16.7 at.%. Interestingly, however, while the drop in nitric oxide oxidation efficiency (ξ_{NO}) was decreased by a factor of about 5 to 15, the efficiency in total nitrogen oxide removal (ξ_{NOx}) was only smaller by a factor of about 3 to 6, indicating that the spectrum of the formed products is significantly altered in the co-doped materials.

This highlights that absolute activity should not be the only factor to consider when evaluating photocatalyst performance. The photocatalytic oxidation of nitric oxide to nitrate involves several intermediate steps, most notably the formation of nitrogen dioxide before it is finally fully oxidised to nitrate. Nitrogen dioxide, however, is a strong environmental pollutant itself.

To account for this, nitrogen dioxide levels were also monitored during the photocatalytic reaction and catalyst selectivity for nitrate (S) is introduced as an additional parameter. The selectivity expresses the ratio of degraded NO that ends up as innocuous nitrate rather than toxic nitrogen dioxide and is derived according to eq. 3.

$$S = \frac{\xi_{NOx}}{\xi_{NO}} \quad (3)$$

As evident in Figure 2, the selectivity gradually rises with increasing tungsten content. This is true for both the samples doped with tungsten and the ones codoped with tungsten and nitrogen. A significant increase in the selectivity can first be observed at a tungsten loading of 2 at.%. At tungsten loadings of 4.8 at.% or higher, no significant further improvement in the selectivity is observed, even when increasing the tungsten-doping ratio to 16.7 at.%. Instead, all of the samples with high tungsten concentration display more or less the same high selectivity of 82 to 91 %.

Furthermore, the results were empirically fit with an exponential decay function (eq. 4, best fit: $y_0 = 1.560 \times 10^{-4}$, $A_1 = 5.186 \times 10^{-4}$, $t_1 = 0.0038$) for the activity and an asymptotic function (eq. 5, best fit: $a = 0.91803$, $b = 0.71592$, $c = 2.101 \times 10^{-11}$) for the selectivity, respectively. With these empirical functions, a good fit for the experimental data was obtained with deviations within the expected experimental errors.

$$y = y_0 + A_1 \cdot e^{-x/t_1} \quad (4)$$

$$y = a - b \cdot c^x \quad (5)$$

These materials were produced using a lab-scale sol-gel synthetic process which is expensive and difficult to scale up.

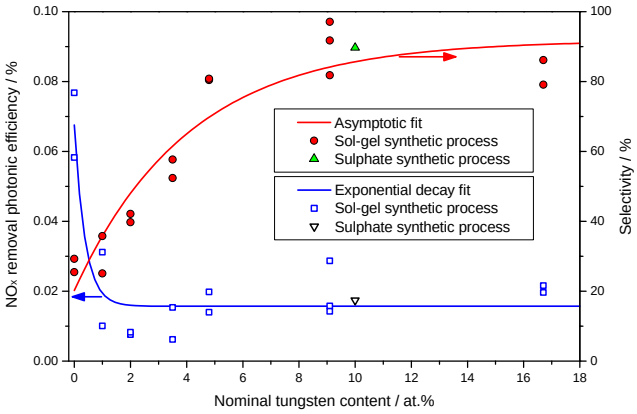

Fig. 2 Photocatalytic activity for the removal of NO_x, expressed as photonic efficiency (left axis, blue open squares) and the selectivity of the reaction with respect to nitrate formation (right axis, red filled circles) in relation to the nominal tungsten content of the material. Plotted are the tungsten-nitrogen co-doped TiO_2 samples as well as the purely tungsten doped one. In addition to the sol-gel derived samples there is also a sample synthesised using the sulphate process (PC7A, green and black triangle)

We were, however, able to obtain a W/N-codoped sample with 10 at.% W loading from Huntsman Pigments that was produced using the same sulphate synthetic process commonly used for large-scale TiO_2 production. This sample, denoted PC7A, showed almost exactly the same behaviour in both activity and selectivity as the sol-gel derived samples with similar tungsten loading, proving that these materials can readily be scaled up and produced with established industrial processes.

In order to ascertain that the observed effects are not related to the photocatalyst surface being completely saturated with nitrate, the time at which such a saturation would occur was calculated. It has been shown that nitrate saturation occurs at approximately 2 molecules per square nanometre of photocatalyst surface and that nitrate can freely diffuse into layers not exposed to light so that saturation is only reached when the whole amount of photocatalyst is completely saturated at 2 nm^{-2}.[44] Under the conditions employed, this saturation would be reached at approximately 1 h g m^{-2} multiplied by the specific surface area of the material, assuming a complete conversion of all nitric oxide to nitrate. Considering that both, the specific surface area of the samples was at least 10 $m^2\ g^{-1}$ and the conversion to nitrate was considerably less than 50 % in all cases, it is highly unlikely that nitrate saturation did occur within the maximum of 20 h the experiments were conducted.

Table 1 Measured activity data for both, the reference materials and the ones synthesised in this work. Listed are the phase of the material as already reported elsewhere[32] (A = anatase, B = brookite, R = rutile), the photonic efficiencies for the removal of total NO_x (ξ_{NOx}) and NO (ξ_{NO}) and the evolution of NO_2 (ξ_{NO2}) as well as the calculated quantities nitrate selectivity (S) and DeNOx index (ξ_{DeNOx})

Sample	Phase / %	S / %	ξ_{DeNOx} / ppm	ξ_{NOx} / ppm	ξ_{NO} / ppm	ξ_{NO2} / ppm
Aeroxide P25	75A/25R	27.8	−3689	878	3162	2284
Aeroxide P90	90A/10R	26.8	−3163	710	2647	1937
UV100	100A	27.2	−3928	900	3314	2414
PC50	100A	25.1	−2129	429	1708	1279
PC105	100A	29.1	−4090	1054	3627	2572
PC500	100A	28.8	−3543	897	3117	2220
Rutile TiO_2	100R	6.9	−232	9	129	120
Brookite TiO_2	100B	38.8	−2952	1374	3537	2163
W-0-400	70A/30B	27.8	−2273	541	1974	1407
W-0-600	28A/72R	7.5	−1823	77	1026	950
W-0-800	100R	6.3	−1218	42	672	630
WN-0-400	100A	29.3	−2940	768	2622	1854
WN-0-600	96A/4R	9.4	−3938	217	2294	2077
WN-0.1-400	100A	29.1	−1483	382	1315	933
WN-0.1-600	88A/12R	13.6	−1494	127	938	811
WN-0.5-400	100A	24.1	−1598	302	1251	950
WN-0.5-600	100A	24.7	−777	152	617	465
WN-1.0-400	100A	25.1	−500	101	401	301
WN-1.0-600	100A	25.0	−996	199	796	598
WN-2.0-400	100A	39.8	−168	83	208	128
WN-2.0-600	100A	42.1	−132	75	179	104
WN-3.5-400	100A	57.7	−72	153	266	112
WN-3.5-600	100A	52.4	−51	62	118	56
WN-4.8-400	100A	80.8	73	140	173	33
WN-4.8-600	100A	80.4	101	198	246	48
WN-9.1-400	100A	81.8	79	142	174	32
WN-9.1-600	100A	97.1	148	158	162	5
W-9.1-600	98A/2R	91.7	235	287	312	26
WN-16.7-600	100A	86.1	133	196	228	32
PC7A (10% W)	100A	89.7	134	174	194	20

4 Discussion

The systematic testing of different titanium dioxide based photocatalysts revealed that in addition to different rates of reaction, *i.e.*, photocatalytic activity, some catalysts also produce a different spectrum of products. This feature can be easily expressed as the selectivity of the reaction with respect to nitrate formation. A high selectivity means that almost all NO is completely oxidised to nitrate before being released into the environment and that NO_2 release is strongly suppressed. The results of the pure titanium dioxide samples serve to highlight the discussed problem very well, as the main product of their photocatalytic reaction with NO is NO_2. This is especially true for the samples containing rutile, suggesting that the presence of this phase is detrimental to the selectivity. These findings are consistent with other reports on photocatalytic NO_x abatement[28,45–55] which also report significant NO_2 evolution upon NO oxidation, although the consequences of this observation, that these catalysts could potentially increase the air toxicity rather than decrease it, are usually not discussed.

However, as illustrated in Figure 2, the increased selectivity is bought at the expense of activity which decreases in turn as the selectivity increases. In terms of conversion to nitrate (ξ_{NOx}), the activity at higher tungsten content drops to only about a third of its original value.

The existence of two individual parameters - activity on one side and selectivity on the other - makes an unambiguous evaluation of the catalysts exceedingly difficult, especially in this case, where their trends work in conflicting directions. As a solution to this, we propose to introduce an alternative way to rate and evaluate photocatalysts in their nitrogen oxide abatement performance, the *DeNOx index* (ξ_{DeNOx}). Rather than looking at the concentration changes of the individual nitrogen oxide species, this index assesses the change in total nitrogen oxide associated toxicity. However, in order to achieve this, relative toxicity values need to be assigned to the individual species.

Relative toxicity assessment of the NO_x gases

Because both nitric oxide and nitrogen dioxide are very much entwined in atmospheric chemistry, it is difficult to assign exact values for their relative danger. Unfortunately, while there is information available on acute and chronic toxicity of both compounds at higher concentrations, there is virtually no significant data available on the long-term effects of ambient level exposure to NO and NO_2. The danger of nitrogen oxides on human health at ambient concentrations is instead derived from epidemiological studies.[56,57] Thus, it is difficult to say how much more dangerous NO_2 actually is when compared to NO in long term chronic exposure to low levels. Here, we arbitrarily assign a relative toxicity value of 1 to NO and 3 to NO_2. We base this evaluation on the following considerations.

Nitric oxide is considered a dangerous compound mainly for its tendency to form the toxic nitrogen dioxide, while it is not so harmful itself. In fact, air quality regulations such as the EU Directive 2008/50/EC usually only set limit thresholds for NO_2, not for NO.[4] The OSHA, ACGIH and NIOSH all place the limit value of NO at 25 ppm.[58] Nitrogen dioxide, on the other hand, is a dangerous compound for several reasons. First of all, it has a much lower toxic concentration for humans and animals, both, in acute in chronic exposure. The limit value on NO_2 varies from 1 to 3 ppm, making it 8 to 25 times more dangerous than NO.[58] Also, as a result of its photolysis followed by reaction with molecular oxygen, it may form ozone, which is even more toxic with a limit value of 0.1 ppm.[58] In fact, the photolysis of nitrogen dioxide is the major source of ozone found at ground level. Until eventually stopped by the oxidation of NO_2 to nitrate, which is rather slow in comparison, this NO-NO_2-cycle continues, forming ozone in the process.[59] Photocatalysis offers a convenient approach to skip the NO_2 intermediate and fast forward to nitrate instead, avoiding the formation of ozone altogether. However, this can only be achieved when the catalyst has a high selectivity towards nitrate. With a low selectivity and consequently high nitrogen dioxide formation level, the photocatalyst would actually even amplify the adverse effects of NO_x by speeding up the first part of the reaction, the oxidation of NO to NO_2. This also raises the question of why NO_x abatement is commonly assessed only on the basis of NO removal rather than NO_2 or total NO_x removal.[29]

Given the relative toxicity of 8 to 25 for higher concentrations and the additional risk of ozone formation, the assumption that NO_2 contributes three times as much as NO to the NO_x-associated air toxicity seems a conservative estimate. The DeNOx index can then be calculated according to eq. 6 or eq. 7, where ξ_{NO} and ξ_{NO2} represent the photonic efficiencies of NO removal and NO_2 formation, respectively, and S the selectivity towards nitrate formation according to eq. 3.

$$\xi_{DeNOx} = \xi_{NO} - 3 \cdot \xi_{NO2} \quad (6)$$

$$\xi_{DeNOx} = \xi_{NOx} \cdot (3 - \frac{2}{S}) \quad (7)$$

This index is dimensionless and will be positive if the catalyst lowers the overall NO_x toxicity, according to the above-mentioned weighing, and negative if the catalyst increases the toxicity level. The threshold for a positive index is a nitrate selectivity of at least 66.7 %. It should be noted that using the index in combination with a test that uses pure NO as the pollutant gas overemphasises the possible adverse effects since in real world conditions, there is always a mixture of both NO and NO_2 present, typically in roughly similar concentrations.[8,60,61] This means that while an unselective photocata-

lyst evolves a lot of NO_2 by oxidising NO, it also oxidises some of the NO_2 already present, so the overall NO_2 concentration might not change considerably at all or at least not as much as the present studies on pure NO might suggest. This behaviour is indicated by systematic studies on the photocatalytic abatement of different NO/NO_2-mixtures using P25 as a photocatalyst.[46] However, this does not change the fact that a more selective catalyst will still perform better in these conditions as it will both oxidise the already present NO_2 and the NO while avoiding to release any additional NO_2, resulting in an overall reduction in the NO_2-level.

Many of the tested samples including all reference materials exhibit a selectivity of 30 % or less, reflecting an unfavourable, negative DeNOx index. Systems characterised by very high activity but inadequate selectivity ($\leq 50\,\%$) could potentially increase the air toxicity by predominant formation of NO_2 rather than decreasing it. Only the samples with a tungsten content of 4.8 at.% or more displayed a significantly higher selectivity, in the range of 80 to 100 %. Consequently, these samples should in general be preferred in real world applications even though their absolute activity is lower than that of the unmodified photocatalysts.

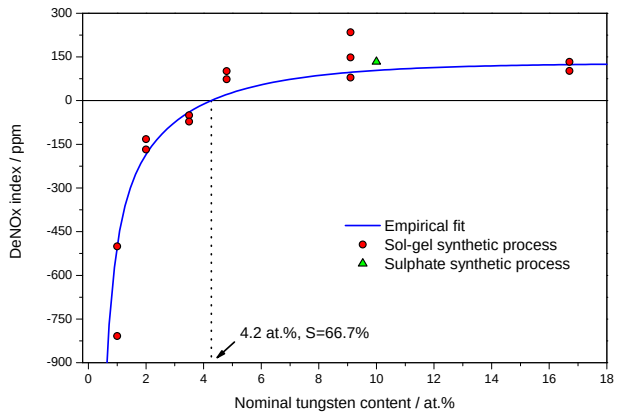

Fig. 3 The DeNOx index as calculated according to eq. 6 for the W-doped and W/N-codoped titanium dioxide photocatalysts in dependence of their tungsten content. Displayed are the measured data points for the sol-gel derived samples (red dots) and the W/N-codoped TiO_2 derived from the sulphate process (PC7A, green triangle) as well as the empirical fit from Figure 2 (blue line)

Using the empirical fit functions for activity and selectivity, eqs. 4 and 5, the resulting DeNOx index can be calculated as well according to eq. 7 (see solid line in Figure 3) and the tungsten content at which the DeNOx index turns positive ($S \geq \frac{2}{3}$) estimated at 4.2 at.%. This is in accordance with the experimental results where the samples with 3.5 at.% or less tungsten have a negative DeNOx index but the ones with 4.8 at.% tungsten or higher are all positive. At high tungsten concentrations the DeNOx index is virtually constant and no further improvement is observed upon addition of more than 9.1 at.% tungsten.

When the pure titanium dioxides are considered, it appears that all materials based exclusively on anatase exhibit a very reproducible selectivity of 24 to 29 %, independent of their particle size, surface area and synthesis method. This is also the case for the co-doped materials with a tungsten content low enough to not yet induce an increased selectivity, *i.e.*, $\leq 1\,\%$. Likewise, pure rutile powders show a much lower selectivity of 6 to 7 %. These results suggest that the selectivity is a fundamental property of the material and that anatase is much more selective than rutile. When mixed phases are considered, a diverging behaviour is observed for some of the materials, as shown in Figure 4. The Aeroxide titanium dioxide particles exhibit the same selectivity as is seen for pure anatase, even though they also contain 10 to 25 % of rutile. However, when the co-doped powders with a low ($\leq 1\,\%$) tungsten content are studied, those with even a very small amount of rutile show a drastically reduced selectivity, more in line with what was observed in the pure rutile powders. This may be a consequence of the different synthetic route, as the Aeroxides are produced by flame pyrolysis and the co-doped powders were obtained in a sol-gel synthesis. In fact, the atypical behaviour of the Aeroxides, mainly P25, has already been reported for several other properties, such as their unusually high photocatalytic activity.

It should also be noted that the brookite powder tested here for comparison displays a significantly higher selectivity than the other titanium dioxide phases, 38.8 %. However, due to the difficulty in obtaining brookite as a pure phase and the unavailability of it as a commercial product, we were not yet able to confirm this value with different brookite powders.

The selectivity of the reaction is most likely a property of both the photocatalyst and the experimental setup used. Our results presented herein show that the selectivity of a given material, *e.g.*, anatase or rutile, is reproducible within a very small experimental error and no dependence on the surface area, particulate size or absolute photocatalytic activity was observed. In the experimental setup, parameters such as initial concentration of the pollutant gases, gas flow rate and residence time, mass of catalyst used and the irradiance of the light source are expected to have an influence on the selectivity. However, while not showing the exact same value, the low selectivity of ordinary anatase photocatalysts was observed without exception in the variety of different experimental setups that have been reported, including that of the widely used ISO 22197-1 standard.[11,27,43,45–55] Consequently, the selectivity must be a feature attributable mainly to the material used as photocatalyst.

At present, we do not yet understand the mechanism of the increased selectivity. Possible causes should be investigated

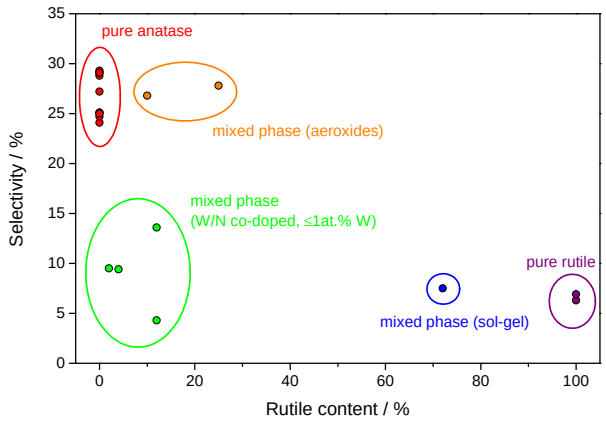

Fig. 4 The selectivity of the photocatalytic reaction with respect to nitrate formation versus the rutile content in the phase composition. Plotted are all reference materials and all of the W/N codoped materials with a tungsten content of 1 at.% or less. The data points are coloured according to their compositions: pure anatase in red, pure rutile in purple, mixed phase (Aeroxides, P25 and P90) in orange, mixed phase (W/N-codoped) in green and mixed phase (sol-gel, no doping) in blue

in the different properties of the modified materials and will be the focus of future studies. These include an altered surface chemistry and acidity, compositional heterogeneity, including surface concentration of specific phases, conduction band position and electron transfer reactions and changes in the adsorption capabilities.

5 Conclusions

It has been known and reported for some time that while titanium dioxide has the potential to photocatalytically oxidise nitric oxide to nitrate, it also releases a significant amount of the toxic intermediate nitrogen dioxide in the process. Even so, the implications of this observation are usually not discussed. Instead, most authors only report activity as the sole figure of merit and do not mention or discuss selectivity at all. However, a poorly selective photocatalyst has the potential to increase the adverse effects of air pollution rather than decrease it by releasing vast amounts of the toxic nitrogen dioxide - this is why the selectivity matters and cannot be ignored. As a possible solution to the problem, the photocatalytic performance of a previously developed W/N-codoped titanium dioxide is reported which has the potential to eliminate this unwanted side-effect.

It was shown that several of the novel compositions significantly outperform conventional photocatalysts in terms of their nitrate selectivity. The selectivity appears to be solely dependent on the tungsten doping ratio and independent of nitrogen codoping or calcination temperature. A tungsten concentration of 4.8 at.% is sufficient to induce a high selectivity and is not further improved by adding even more tungsten. The high selectivity could also be replicated by a W/N-codoped sample derived from the industrial sulphate synthetic process.

The mechanistic pathway for the increased nitrate selectivity has not as yet been elucidated and will be the focus of future studies on these materials. This is considered to be the first report of selective photocatalytic oxidation of nitric oxide to nitrate using titanium dioxide based materials. Minimising the production of NO_2 in the catalytic process has significant environmental and public health implications and has not been specifically addressed previously in the photocatalytic literature. This property highlights a significant differentiator between the novel W/N-doped catalysts and conventional TiO_2-based catalysts.

However, this increased selectivity is accompanied by a decrease in absolute photocatalytic activity by a factor of about 3. This raises the question of how to properly evaluate NO_x abatement photocatalysts when there are two figures of merit to consider, activity and selectivity.

By distilling total NO_x removal and selectivity into one value, we propose to define a DeNOx index (ξ_{DeNOx}) for the evaluation of NO_x abatement photocatalysts. It is derived by assigning a toxicity value to both NO and NO_2 and then expressing the change in total toxicity rather than the change in the individual nitrogen species. The DeNOx index represents the relative change in nitrogen oxide associated air toxicity, defined by the weighing factors of 1 and 3 for NO and NO_2, respectively, that is caused by the photocatalyst upon illumination. At this point this is an arbitrary assignment since exact toxicity data for long term chronic exposure at the low ambient concentrations are not available, but given the relative toxicity at higher concentrations this seems a conservative estimate. Not only does this new index allow for a better evaluation of the NO_x removal properties of photocatalysts, it also reduces the amount of data to process, allowing for a clearer picture of the situation.

Acknowledgement

The work reported in this paper has been funded by the European Union's Seventh Framework Programme (FP7) Project Light^{2}Cat (Grant No. 283062, Theme Environment).

References

1 K. Skalska, J. S. Miller and S. Ledakowicz, *The Science of the Total Environment*, 2010, **408**, 3976–89.

2 U. Gehring, O. Gruzieva, R. M. Agius, R. Beelen, A. Custovic, J. Cyrzs, M. Eeftens, C. Flexeder, E. Fuertes, J. Heinrich, B. Hoffmann, J. C. de Jongste, M. Kerkhof, C. Klümper, M. Korek, A. Mölter, E. S. Schultz,

A. Simpson, D. Sugiri, M. Svartengren, A. von Berg, A. H. Wijga, G. Pershagen and B. Brunekreef, *Environmental Health Perspectives*, 2013, **121**, 1357–1364.

3 B. Chen, C. Hong and H. Kan, *Toxicology*, 2004, **198**, 291–300.

4 The European Parliament and the Council of the European Union, *Official Journal of the European Union*, 2008, **L152**, 1–44.

5 G. Fontaras, V. Franco, P. Dilara, G. Martini and U. Manfredi, *The Science of the Total Environment*, 2014, **468-469**, 1034–42.

6 J. Lasek, Y.-H. Yu and J. C. Wu, *Journal of Photochemistry and Photobiology C: Photochemistry Reviews*, 2013, **14**, 29–52.

7 M. L. Williams and D. C. Carslaw, *Atmospheric Environment*, 2011, **45**, 3911–3912.

8 R. Kurtenbach, J. Kleffmann, A. Niedojadlo and P. Wiesen, *Environmental Sciences Europe*, 2012, **24**, 21.

9 R. De_Richter and S. Caillol, *Journal of Photochemistry and Photobiology C: Photochemistry Reviews*, 2011, **12**, 1–19.

10 A. Folli, C. Pade, T. B. k. Hansen, T. De Marco and D. E. Macphee, *Cement and Concrete Research*, 2012, **42**, 539–548.

11 S. Laufs, G. Burgeth, W. Duttlinger, R. Kurtenbach, M. Maban, C. Thomas, P. Wiesen and J. Kleffmann, *Atmospheric Environment*, 2010, **44**, 2341–2349.

12 G. Hüsken, M. Hunger and H. Brouwers, *Building and Environment*, 2009, **44**, 2463–2474.

13 C. Guo, X. Wu, M. Yan, Q. Dong, S. Yin, T. Sato and S. Liu, *Nanoscale*, 2013, **5**, 8184–91.

14 S. Hanson, P. Tikalsky and F. Asce, *Journal of Materials in Civil Engineering*, 2013, **25**, 893–898.

15 R. Sugrañez, J. Álvarez, M. Cruz-Yusta, I. Mármol, J. Morales, J. Vila and L. Sánchez, *Building and Environment*, 2013, **69**, 55–63.

16 J. Chen, S.-c. Kou and C.-s. Poon, *Building and Environment*, 2011, **46**, 1827–1833.

17 M. Chen and Y. Liu, *Journal of Hazardous Materials*, 2010, **174**, 375–9.

18 M. Chen and J.-W. Chu, *Journal of Cleaner Production*, 2011, **19**, 1266–1272.

19 M. Ballari and H. Brouwers, *Journal of Hazardous Materials*, 2013, **254-255**, 406–14.

20 G. L. Guerrini, *Construction and Building Materials*, 2012, **27**, 165–175.

21 T. Maggos, A. Plassais, J. Bartzis, C. Vasilakos, N. Moussiopoulos and L. Bonafous, *Environmental Monitoring and Assessment*, 2008, **136**, 35–44.

22 T. Maggos, J. G. Bartzis, M. Liakou and C. Gobin, *Journal of Hazardous Materials*, 2007, **146**, 668–73.

23 A. Folli, J. Z. Bloh, M. Strøm, T. Pilegaard Madsen, T. Henriksen and D. E. Macphee, *The Journal of Physical Chemistry Letters*, 2014, **5**, 830–832.

24 A. Hakki, R. Dillert and D. W. Bahnemann, *Physical Chemistry Chemical Physics*, 2013, **15**, 2992–3002.

25 T. Zhang, L. You and Y. Zhang, *Dyes and Pigments*, 2006, **68**, 95–100.

26 A. V. Emeline, V. N. Kuznetsov, V. K. Ryabchuk and N. Serpone, *Environmental Science and Pollution Research*, 2012, **19**, 3666–75.

27 J. Ma, H. Wu, Y. Liu and H. He, *The Journal of Physical Chemistry C*, 2014, **118**, 7434–7441.

28 J. Ângelo, L. Andrade and A. Mendes, *Applied Catalysis A: General*, 2014.

29 S. Ifang, M. Gallus, S. Liedtke, R. Kurtenbach, P. Wiesen and J. Kleffmann, *Atmospheric Environment*, 2014, **91**, 154–161.

30 J. Z. Bloh, R. Dillert and D. W. Bahnemann, *Physical Chemistry Chemical Physics*, 2014, **16**, 5833–5845.

31 N. Todorova, T. Vaimakis, D. Petrakis, S. Hishita, N. Boukos, T. Giannakopoulou, M. Giannouri, S. Antiohos, D. Papageorgiou, E. Chaniotakis and C. Trapalis, *Catalysis Today*, 2013, **209**, 41–46.

32 J. Z. Bloh, A. Folli and D. E. Macphee, *The Journal of Physical Chemistry C*, 2014, accepted manuscript.

33 T. A. Kandiel, L. Robben, A. Alkaim and D. Bahnemann, *Photochemical & Photobiological Sciences*, 2013, **12**, 602–609.

34 T. A. Kandiel, A. Feldhoff, L. Robben, R. Dillert and D. W. Bahnemann, *Chemistry of Materials*, 2010, **22**, 2050–2060.

35 C. A. Parker, *Proceedings of the Royal Society A: Mathematical, Physical and Engineering Sciences*, 1953, **220**, 104–116.

36 C. G. Hatchard and C. A. Parker, *Proceedings of the Royal Society A: Mathematical, Physical and Engineering Sciences*, 1956, **235**, 518–536.

37 J. Ângelo, L. Andrade, L. M. Madeira and A. Mendes, *Journal of Environmental Management*, 2013, **129**, 522–39.

38 R. Dillert, J. Stötzner, A. Engel and D. W. Bahnemann, *Journal of Hazardous Materials*, 2012, **211-212**, 240–6.

39 R. Dillert, A. Engel, J. Große, P. Lindner and D. W. Bahnemann, *Physical Chemistry Chemical Physics*, 2013, **15**, 20876–86.

40 D. Gray, E. Lissi and J. Heicklen, *The Journal of Physical Chemistry*, 1972, **76**, 1919–1924.

41 E. B. Myers and T. J. Overcamp, *Environmental Engineering Science*, 2002, **19**, 321–327.

42 J. A. Rodriguez, T. Jirsak, G. Liu, J. Hrbek, J. Dvorak and A. Maiti, *Journal of the American Chemical Society*, 2001, **123**, 9597–605.

43 Y.-M. Lin, Y.-H. Tseng, J.-H. Huang, C. C. Chao, C.-C. Chen and I. Wang, *Environmental Science & Technology*, 2006, **40**, 1616–21.

44 Y. Ohko, Y. Nakamura, A. Fukuda, S. Matsuzawa and K. Takeuchi, *The Journal of Physical Chemistry C*, 2008, **112**, 10502–10508.

45 M. Ballari, M. Hunger, G. Hüsken and H. Brouwers, *Catalysis Today*, 2010, **151**, 71–76.

46 M. Ballari, Q. Yu and H. Brouwers, *Catalysis Today*, 2011, **161**, 175–180.

47 M.-V. Sofianou, V. Psycharis, N. Boukos, T. Vaimakis, J. Yu, R. Dillert, D. Bahnemann and C. Trapalis, *Applied Catalysis B: Environmental*, 2013, **142-143**, 761–768.

48 B. N. Shelimov, N. N. Tolkachev, O. P. Tkachenko, G. N. Baeva, K. V. Klementiev, A. Y. Stakheev and V. B. Kazansky, *Journal of Photochemistry and Photobiology A: Chemistry*, 2008, **195**, 81–88.

49 S. Devahasdin, C. Fan, K. Li and D. H. Chen, *Journal of Photochemistry and Photobiology A: Chemistry*, 2003, **156**, 161–170.

50 A. Folli, S. B. Campbell, J. a. Anderson and D. E. Macphee, *Journal of Photochemistry and Photobiology A: Chemistry*, 2011, **220**, 85–93.

51 E. Luévano-Hipólito, a. M.-d. L. Cruz, Q. Yu and H. Brouwers, *Applied Catalysis A: General*, 2013, **468**, 322–326.

52 Y. Ohko, Y. Nakamura, N. Negishi, S. Matsuzawa and K. Takeuchi, *Journal of Photochemistry and Photobiology A: Chemistry*, 2009, **205**, 28–33.

53 Q. Wu and R. van de Krol, *Journal of the American Chemical Society*, 2012, **134**, 9369–75.

54 M. Polat, A. M. Soylu, D. a. Erdogan, H. Erguven, E. I. Vovk and E. Ozensoy, *Catalysis Today*, 2014, 1–8.

55 N. Todorova, T. Giannakopoulou, S. Karapati, D. Petridis, T. Vaimakis and C. Trapalis, *Applied Surface Science*, 2014.

56 P. E. Morrow, *Journal of Toxicology and Environmental Health*, 1984, **13**, 205–27.

57 V. Mohsenin, *Toxicology*, 1994, **89**, 301–12.

58 R. J. Lewis and N. I. Sax, *Sax's Dangerous Properties of Industrial Materials*, Van Nostrand Reinhold, New York, 9th edn, 1996.

59 Y. Sadanaga, J. Matsumoto and Y. Kajii, *Journal of Photochemistry and Photobiology C: Photochemistry Reviews*, 2003, **4**, 85–104.

60 A. Chaney, D. Cryer, E. Nicholl and P. Seakins, *Atmospheric Environment*, 2011, **45**, 5863–5871.

61 Z.-H. Shon, K.-H. Kim and S.-K. Song, *Atmospheric Environment*, 2011, **45**, 3120–3131.

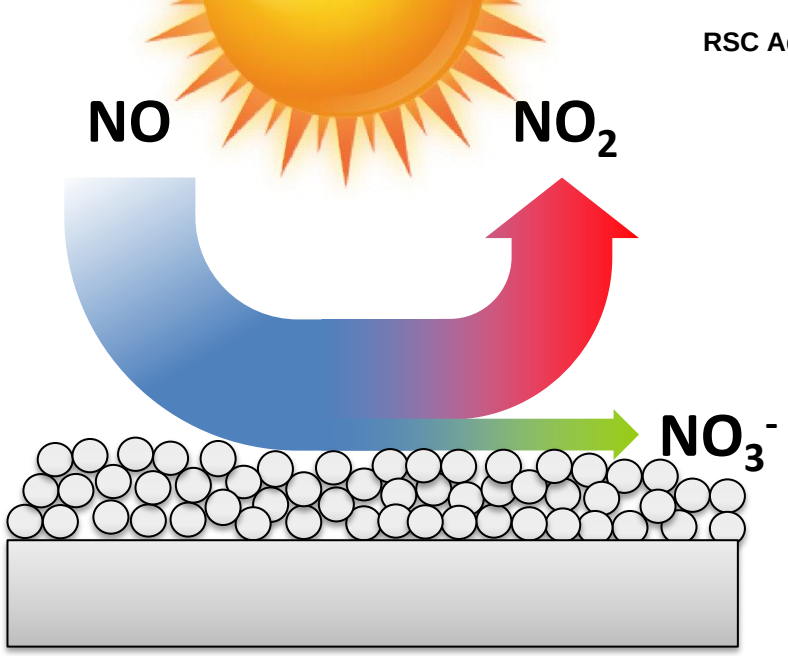

Ordinary TiO_2
low selectivity

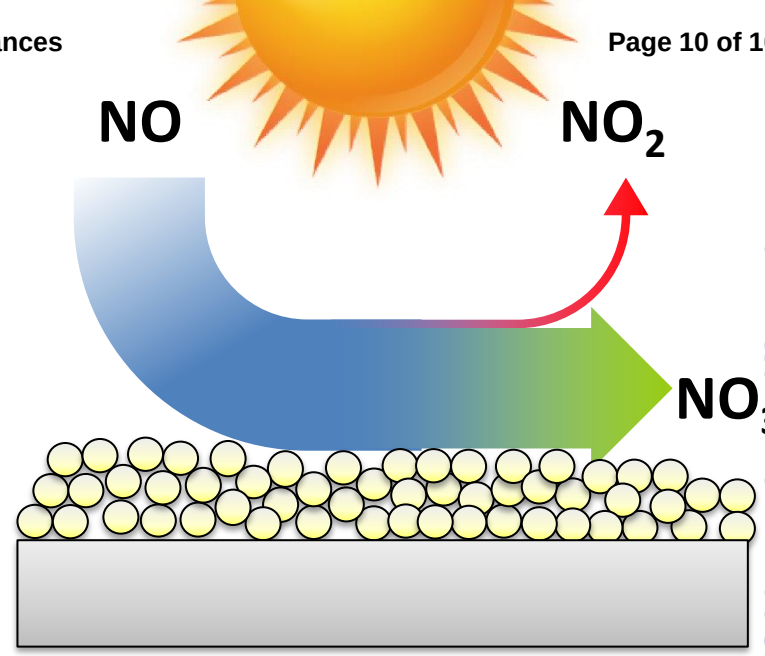

W/N-codoped TiO_2
high selectivity